

Determining Required Surveillance Performance for Unmanned Aircraft Sense and Avoid*

Matthew W. M. Edwards[†] and Justin K. Mackay[‡]

Lincoln Laboratory, Massachusetts Institute of Technology, Lexington, MA 02420

Sense and avoid is the unmanned aircraft system capability to comply with the regulatory requirement to see and avoid other aircraft. A key challenge to developing an acceptable sense and avoid system is the surveillance subsystem that must sense and track a variety of potentially threatening aircraft. Determining the required surveillance performance is not straightforward due to the complex interaction of surveillance performance with other system components to affect collision risk. This is typically accomplished using high-fidelity, fast-time, sample-based simulation that requires long development and analysis timelines, where the computational burden is high. This work provides an analytic approach to map surveillance performance to collision risk that mitigates these resource requirements in several cases. This approach is demonstrated when encountering noncooperative, or nontransponding, aircraft which is a key sense and avoid challenge because existing collision avoidance technology relies on cooperative surveillance.

Nomenclature

s	Separation, ft
θ	Azimuth, rad
ϕ	Elevation, rad
ψ	Heading, rad
r	Range, NM
t	Time, s
v	Velocity, kt
σ	Standard Deviation

Subscript

h	Horizontal
v	Vertical
r	Relative
o	Own Aircraft
i	Intruder Aircraft
a	Actual/True
e	Error
p	Predicted
c	Conflict
d	Desired/Goal
m	Maneuverability/Achievable Separation
b	Missed Detection Threshold
n	Nuisance Alert Threshold

*DISTRIBUTION STATEMENT A: Approved for public release; distribution is unlimited; 7 Nov 2016; 2016-860
This material is based upon work supported by the Department of the Navy under Air Force Contract No. FA8721-05-C-0002
and/or FA8702-15-D-0001. Any opinions, findings, conclusions or recommendations expressed in this material are those of the
author(s) and do not necessarily reflect the views of the Department of the Navy.

Copyright © 2018 by Massachusetts Institute of Technology.

Delivered to the U.S. Government with Unlimited Rights, as defined in DFARS Part 252.227-7013 or 7014 (Feb 2014). Notwithstanding any
copyright notice, U.S. Government rights in this work are defined by DFARS 252.227-7013 or DFARS 252.227-7014 as detailed above. Use of this
work other than as specifically authorized by the U.S. Government may violate any copyrights that exist in this work.

[†]Technical Staff, Surveillance Systems, Senior Member.

[‡]Associate Staff, Surveillance Systems.

I. Introduction

Sense and avoid (SAA) is the capability of an unmanned aircraft system (UAS) to comply with the regulatory requirement for aircraft to see and avoid other aircraft (14 CFR §91.111 and §91.113). See and avoid, and thus SAA, is the last line of defense before collision, and is therefore implemented after other modes of separation have been compromised. SAA is minimally comprised of a surveillance system to detect and track other aircraft, and a threat detection and resolution capability that may have varying levels of autonomy: on separate ends of the autonomy spectrum the pilot manually or the computer automatically identifies and resolves threats. Before technologies can be appropriately developed, certified, and deployed, requirements must be decomposed with appropriate traceability to system level requirements. However, SAA subsystem requirements are interdependent and also rely on external factors such as own and intruder speeds and platform escape maneuverability—e.g., higher relative speeds will typically require increased detection range. Thus, the subsystem requirements must be coordinated and fully consider these external factors.

Defining and evaluating the entire requirements tradespace has typically not been tractable because of the number of independent factors involved. Requirements development has typically been initiated with a systematic reduction in the tradespace using methods, such as expert opinion and simple time budgets that are unable to simultaneously consider all factors, that may result in solutions that are only locally optimized. For example, surveillance detection range requirements may be derived without considering the impact of surveillance track uncertainty and system transmission latencies. Given the reduced tradespace from this systematic reduction, a simulation is executed to locally tune specific system attributes. Standard practice is to use realistic large-scale Monte Carlo (sample-based) simulation that requires considerable computational and analysis resources such that computing clusters and teams of researchers are typically employed.^{1,2} Given the many possible SAA surveillance modalities, UAS types with varying performance, and operating environments, there is a need for a simpler approach to determining subsystem, and especially surveillance system, requirements. However, Monte Carlo simulation cannot be fully replaced during system development because time varying system characteristics, such as threat detection and resolution logic, can only be represented in such a simulation.

An SAA surveillance system is composed of the sensor that provides a stream of raw measurements and the tracker: the tracker consists of sensor correlation to associate independent measurements from the same target and filtering to smooth raw measurements and to estimate unmeasured parameters. The sensor and tracker are often tightly coupled in order to optimize surveillance system performance. The SAA system designer is concerned with the outputs of the surveillance system and how they impact other downstream components and ultimately end-to-end system efficacy, rather than the attributes of the sensor and tracker themselves. Therefore, requirements are desired to be specified at the surveillance system (filter) output, rather than at the sensor output in order to ensure end-to-end system efficacy.

The objective of this work is to develop an analytic methodology for decomposing system level requirements and attributes into surveillance subsystem requirements. Previous work has considered the surveillance contribution to correct detection and false alert probabilities,³ while this work evaluates the surveillance contribution to collision risk where escape maneuver efficacy at imparting a separation must be considered. The next section details this approach to tracing surveillance requirements to system safety. Then, the example of an unmanned aircraft encountering noncooperative, or nontransponding, traffic is used to demonstrate the approach.

II. Methodology

The key challenge of collision avoidance is maneuvering to overcome the inherent uncertainties in the projection of the future encounter state. These uncertainties include surveillance error, unanticipated intruder aircraft maneuvers, and unanticipated own aircraft and SAA system behavior, such as variable or incorrect pilot response. Although the general approach outlined below could consider all uncertainties, the surveillance uncertainty is of primary concern. Collision risk is the primary metric of interest; however, the system's operational suitability must also be considered else the system may be theoretically safe but of little practical use. The former is solved first in Section A, while the latter is discussed in Section B; the appendix includes corresponding Matlab code. The more general term *conflict* rather than *collision* is used for the remainder of this section in case other outcomes are of interest.

A. Conflict Risk

In order to solve analytically for conflict risk, the avoidance problem is simplified by considering only the separation at closest approach and in one dimension: vertically or horizontally. This simplification assumes that the aircraft will have no separation in the dimension not being considered, and it does not permit consideration of the three-dimensional extent of the conflict definition—e.g., a cylinder that is typically used for evaluation of collision avoidance and separation systems. Furthermore, it is assumed that a single maneuver decision is made during the encounter at a specified time. In this simplified problem, there is an actual separation, s_a , that would occur if the aircraft does not maneuver (also termed the nominal or unmitigated situation) and an error in the predicted separation, s_e . The predicted separation is the system’s estimate of the separation at closest approach without a maneuver: $s_p = s_a + s_e$. Additionally, there is a separation that defines conflict, s_c , the target separation that is desired, s_d , and a separation that can be achieved by the platform as limited by maneuverability, s_m . Because there are two directions for maneuvering in each dimension, up/down vertically or left/right horizontally, the achievable separation is defined as the average magnitude over each direction; the maneuverability and achievable separation is discussed further in Section E.

A system could be designed to maneuver only in one dimension; in this case, accuracy in the nonmaneuvering direction must be sufficient to determine that a conflict exists, but the accuracy does not need to be sufficient for maneuvering. In the nonmaneuvering dimension, a conflict is predicted when separation at closest approach is estimated within s_b . Additionally, it is generally desirable to minimize nuisance alerts: nuisance alerts occur when a conflict is predicted when in fact separation will be adequate. An alert is classified as a nuisance alert when the actual separation would be greater than s_n . This nomenclature is summarized in Table 1; the first three variables are signed (s_a, s_e, s_p), while the others are defined positive.

Table 1. Analytic formulation nomenclature.

Variable	Description
s_a	Actual/true separation
s_e	Separation prediction error
s_p	Predicted separation
s_c	Conflict definition
s_d	Desired separation
s_m	Achievable separation
s_b	Missed detection separation
s_n	Nuisance alert separation

For this formulation, it is assumed that an escape maneuver will be made that achieves the desired separation; if the desired separation cannot be achieved due to maneuverability limitations, the maneuver that maximizes separation will be selected. Achievable separation exceeding the desired separation does not impact the risk. It would seem that maximum separation would always be desirable to reduce risk, however there are operational limitations that must be considered: for example, it is typically undesirable to conflict with aircraft separated at standard airspace vertical separations of 500, 1000, and 2000 ft. As an example of a currently operational system, the Traffic Alert and Collision Avoidance System (TCAS) defines a desired vertical separation, the altitude limit (ALIM), that changes with altitude in order to compensate for barometric altimetry system error but it is limited in order to not conflict with standard cruising altitudes.^{4,5}

Conflict risk is comprised of both induced and unresolved components. Induced risk results from maneuvering into conflict, while unresolved risk is that which the system was not able to overcome. The conflict risk metric used to assess collision avoidance and SAA systems is the risk ratio (RR) which is the fraction of conflicts remaining after implementing the system. For example, a risk ratio of 0.1 would indicate that the system mitigated 90% of the risk that existed before equipping with the system, and the 0.1 risk ratio would

be the aggregate of unresolved and induced risk. The risk ratio as defined for evaluation of collision risk is:

$$\text{Risk Ratio} = \frac{\lambda_{\text{mac}}}{\lambda_{\text{nominal mac}}} \quad (1)$$

$$= \frac{P(\text{mac} | \text{encounter})\lambda_{\text{encounter}}}{P(\text{mac} | \text{nominal encounter})\lambda_{\text{encounter}}} \quad (2)$$

$$\approx \frac{P(\text{nmac} | \text{encounter})}{P(\text{nmac} | \text{nominal encounter})} \quad (3)$$

$$= \frac{P(\text{unresolved nmac} | \text{encounter})}{P(\text{nmac} | \text{nominal encounter})} + \frac{P(\text{induced nmac} | \text{encounter})}{P(\text{nmac} | \text{nominal encounter})}, \quad (4)$$

where λ_{mac} denotes a midair collision (mac) rate while the term *nominal* denotes the situation without the system; when this term (*nominal*) is not used it signifies the situation with the system. A near midair collision (NMAC) is typically used to approximate midair collisions as a modeling convenience so as not to require modeling the complex interaction of aircraft geometries, and to provide statistical confidence for Monte Carlo simulation; this approximation is also conservative in that it overestimates the risk ratio.^{5,6} Although the formal definition of risk ratio is based on midair collisions and near midair collisions as a modeling surrogate, other ratios may be of interest such as for a well clear violation or collision hazard.

An analytic solution to calculating the risk ratio can be determined by evaluating the likelihood of causing a conflict with intruding aircraft that have varying actual separations. Unresolved conflicts can only occur with aircraft that are nominally separated within the conflict definition, while the opposite is true for induced conflicts. Further, induced conflicts can only occur when aircraft are nominally separated within the conflict definition of the desired separation ($s_d + s_c$); otherwise, it is not possible to maneuver into a conflict.

1. Unresolved Risk

An unresolved conflict will occur if the error is such that it appears that no action is necessary ($|s_a + s_e| > s_d$) or a sufficient maneuver is not always implemented ($s_m < 2s_c$). If a sufficient maneuver is implemented ($s_m > 2s_c$) the unresolved risk ratio component is

$$\text{Unresolved Risk Ratio} = \frac{1}{2s_c} 2 \int_0^{s_c} 2 \int_{s_d - s_c}^{\infty} p(s_e) ds_e ds_a \quad (5)$$

$$= 2 \int_{s_d - s_c}^{\infty} p(s_e) ds_e, \quad (6)$$

where it is assumed that the error distribution is independent of the actual relative separation and that the actual relative separation distribution is uniform; otherwise, the integrand would be $p(s_e, s_a)$ and the simplification from Equations 5 to 6 would not be possible. It is also assumed that the error and actual separation distributions are symmetric which results in the factors of two.

When a sufficient maneuver is not implemented ($s_m < 2s_c$), there are maneuvers that could result in an unresolved conflict—as an example, if the actual separation is -75 ft, achievable separation is 150 ft (150 ft climb), and conflict is 100 ft, then an unresolved conflict will occur (resulting separation is 75 ft). As opposed to considering the actual separations that will result in a conflict, the actual separations that will not result in a conflict are considered when estimating unresolved risk with an insufficient maneuver. When $s_m < s_c$, it is only possible to resolve conflict when a maneuver is selected in a direction opposite the intruder's and when $s_a > s_c - s_m$; consequently a conflict will always occur when $s_a < s_c - s_m$. This is represented in Equation 7.

$$\text{Unresolved Risk Ratio } (s_c > s_m) = 1 - \frac{1}{2s_c} 2 \int_{|s_m - s_c|}^{s_c} \int_{-s_a}^{s_d - s_c} p(s_e) ds_e ds_a \quad (7)$$

When $2s_c > s_m > s_c$, a maneuver can always be made to resolve the conflict provided the appropriate surveillance error; this is represented in Equation 8. Notice that Equation 8 extends upon Equation 7 with the last term.

$$\begin{aligned} \text{Unresolved Risk Ratio } (2s_c > s_m > s_c) = & 1 - \frac{1}{2s_c} 2 \int_{|s_m - s_c|}^{s_c} \int_{-s_a}^{s_d - s_c} p(s_e) ds_e ds_a \\ & - \frac{1}{2s_c} 4 \int_0^{|s_m - s_c|} \int_0^{|s_d - s_c|} p(s_e) ds_e ds_a \end{aligned} \quad (8)$$

2. Induced Risk

An induced conflict occurs when the error is such that it causes a maneuver into a conflict; this is typically when $s_d - s_c < |s_e| < s_d + s_c$ (first term in Equation 9). However, when $s_a > s_m - s_c$, this range overlaps the region where a different direction maneuver would be selected (e.g., climb to descend), such that only a portion of the error region will result in an induced conflict (second term).

$$\begin{aligned} \text{Induced Risk Ratio} = & \frac{1}{2s_c} 2 \int_{s_c}^{s_m - s_c} \int_{s_d - s_c}^{s_d + s_c} p(s_e) ds_e ds_a \\ & + \frac{1}{2s_c} 2 \int_{\max(s_m - s_c, s_c)}^{s_m + s_c} \int_{s_a}^{s_d + s_c} p(s_e) ds_e ds_a \end{aligned} \quad (9)$$

The unresolved formulation assumptions apply to this induced formulation as well. If $s_c > s_m - s_c$, then the first term is zero, and the max operator in the second term accounts for the fact that induced conflicts can only occur when the actual separation is greater than the conflict definition ($s_a > s_c$).

3. Missed Detection Rate

For systems that only maneuver in one dimension or for systems where the surveillance information is only used to alert rather than for maneuvering, the ability to predict conflicts in the nonmaneuvering dimension must be considered. A missed detection occurs when a conflict would occur, but it is not predicted:

$$\text{Missed Detection Ratio} = \frac{1}{2s_c} \int_{-s_c}^{s_c} 2 \int_{s_b - s_a}^{\infty} p(s_e) ds_e ds_a. \quad (10)$$

It is assumed that a conflict will not be declared if separation is predicted to be greater than s_b at closest approach. Practically, the missed detection ratio will be similar to the unresolved risk ratio.

B. Alerting Performance

Although conflict risk is of ultimate concern, it is desirable to reduce the alerting rate as low as practicable. Typically, increased alerting will result in reduced risk, at the expense of maneuvering more often. Nuisance alerts, which are alerts that occur during an otherwise safe situation, are of primary interest; however, it is difficult to fully define what constitutes a safe situation (i.e., displacement) such that an alert would be considered unreasonable. Instead, a metric is defined that captures the overall alerting rate: the alert ratio.

1. Alert Rate

Alert ratio is defined in Equation 11 that measures the alerting frequency relative to the unmitigated conflict rate, similar to the risk ratio. Thus, it provides a measure of how often the system alerts relative to how often a conflict would occur without the system.

$$\text{Alert Ratio} = \frac{P(\text{alert} \mid \text{encounter})}{P(\text{conflict} \mid \text{nominal encounter})} \quad (11)$$

The alert ratio can be computed similar to the risk ratio by considering the actual separations that would cause an alert given the surveillance error. An alert will occur when it is assessed that the intruder will pass less than the desired separation (s_d) of the own aircraft, which results in:

$$\text{Alert Ratio} = \frac{1}{2s_c} \int_{-\infty}^{\infty} \int_{s_a - s_d}^{s_a + s_d} p(s_e) ds_e ds_a. \quad (12)$$

When the prediction error distribution, $p(s_e)$, is Gaussian the result is the simple solution that the alert ratio is s_d/s_c . For the nonmaneuvering dimension, s_d can be replaced by s_b .

2. Nuisance Alert Rate

It may be of interest to decompose alerts into nuisance and correct alerts. A nuisance alert, sometimes also called a false alert, is defined as a prediction of conflict where separation would otherwise be sufficient. A nuisance alert could be defined as an alert where a conflict would not have occurred, but due to the required desired separation to account for uncertainty, the nuisance alert rate would seem to be quite high. Typically, a threshold is established larger than the conflict definition to characterize nuisance alerts, which is defined here as s_n : for TCAS, this has been set as a fraction of the air traffic control separation minima.⁷ The nuisance alert ratio is found by considering the actual separations defined as a nuisance that would result in an alert due to prediction error.

$$\text{Nuisance Alert Ratio} = \frac{1}{2s_c} 2 \int_{s_n}^{\infty} \int_{s_a - s_d}^{s_a + s_d} p(s_e) ds_e ds_a. \quad (13)$$

Similar to the total alert rate, s_d can be replaced by s_b in the nonmaneuvering dimension. The difference between the nuisance alert ratio and the total alert ratio is the correct alert ratio.

C. Example Parametric Results

The risk and alert ratio equations formulated above are explicitly solvable when the prediction error can be represented by standard continuous distributions, such as Gaussian and Laplace; the Laplace distribution, also called a double exponential distribution, is often used to represent barometric altimeter errors.⁸ Example risk ratio results for a range of Gaussian distributed prediction error standard deviations and achievable separations are shown in Figure 1, when the desired separation is infinite or 1000 ft. The conflict definition was set at 100 ft which is the vertical NMAC definition used to evaluate TCAS efficacy.⁴ Although impractical, an infinite desired separation results in the minimum achievable risk ratio; this will require a maneuver that maximizes separation regardless of the nominal separation. The unresolved risk ratio is effectively null when the achievable separation exceeds 200 ft, while the induced risk is highest when the prediction error is much larger than the achievable separation.

D. Validation

The analytic solution was validated by executing a simple Monte Carlo simulation. First, a large collection of simplified, single dimension encounters was generated with a range of actual separations at closest approach conforming to a uniform distribution, encompassing all encounters that could result in a conflict. Second, separation error was generated according to the distribution of interest and associated parameters, and then added to the actual separation to calculate the predicted separation. Lastly, a decision was determined based upon the predicted separation: make a maneuver equivalent to the desired separation if achievable, else maximize separation. This was executed for both Gaussian and Laplace separation prediction error distributions, across a range of prediction error standard deviations, achievable separations, and desired separations. The result for a desired separation of 500 ft and Gaussian distributed error is shown in Figure 2; the differences between the analytic and Monte Carlo results are due to sampling error. If the prediction error distribution is not well formed such that an analytic solution does not exist, then this Monte Carlo simulation could be used to evaluate conflict risk.

E. Maneuverability and Achievable Separation

When maneuvering in the vertical dimension, the maneuver magnitude (vertical deviation from course) is able to impart an almost equivalent separation, but this is generally not the case when maneuvering in the horizontal dimension. Take for example crossing geometries where depending on the time to a collision, very little separation can be obtained by turning. The measure to which a separation is induced relative to the maneuver magnitude is termed the maneuver efficiency, and is always less than unity—i.e., the achievable separation cannot be larger than the maneuver displacement. The procedure by which maneuver efficiency can be calculated is described by Morrel.⁹ For arbitrary nominal separation and time, or range, to collision, the relative escape is fixed given the aircraft speeds and relative heading (or bearing). These escape paths are termed cycloids, and an example is shown in Figure 3. The separation during the encounter is the Euclidean distance between the cycloid and the point that represents the escape maneuver decision time and nominal

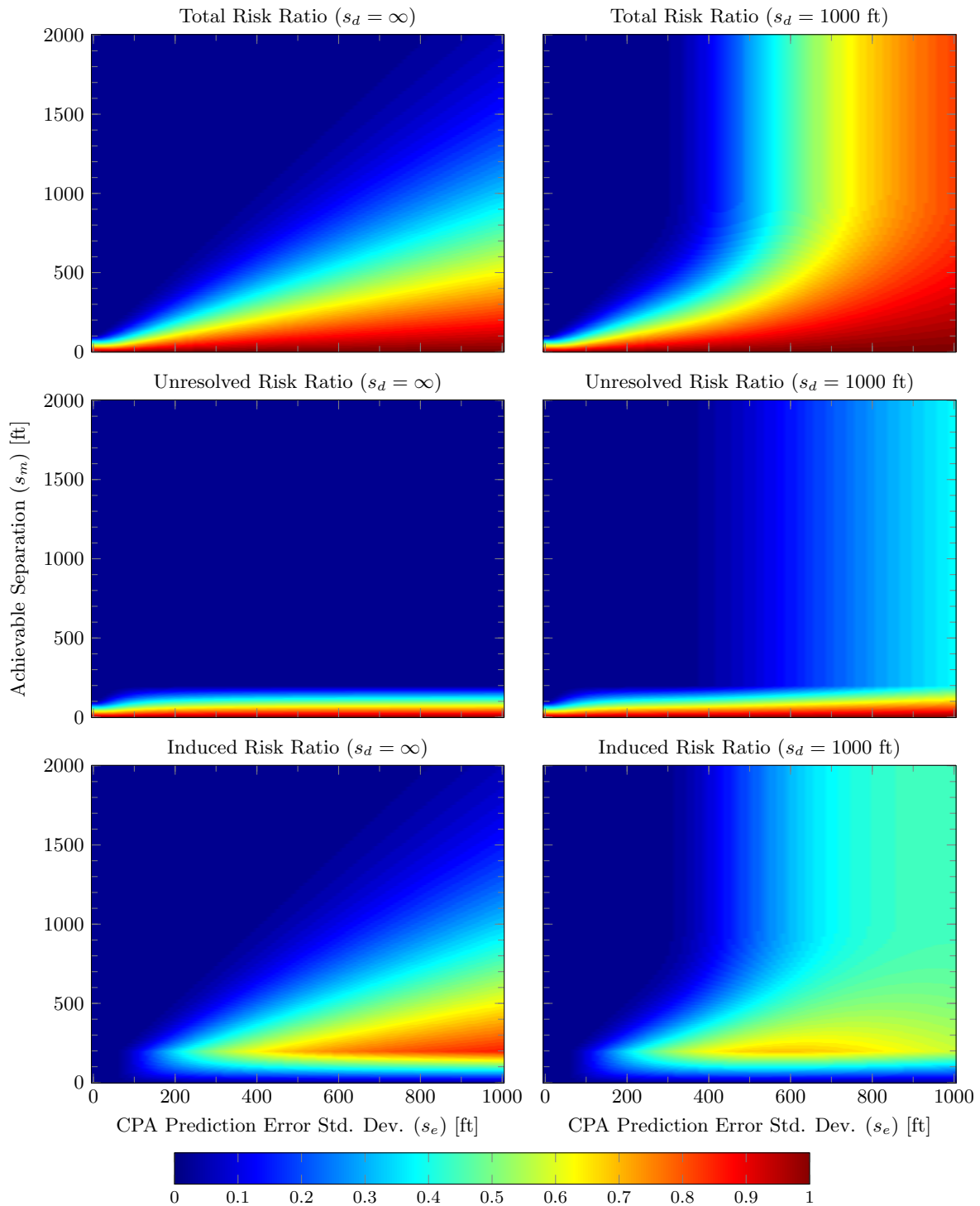


Figure 1. Risk ratio for Gaussian closest approach prediction error for infinite (left) and 1000 ft (right) desired separation, where $s_c = 100$ ft.

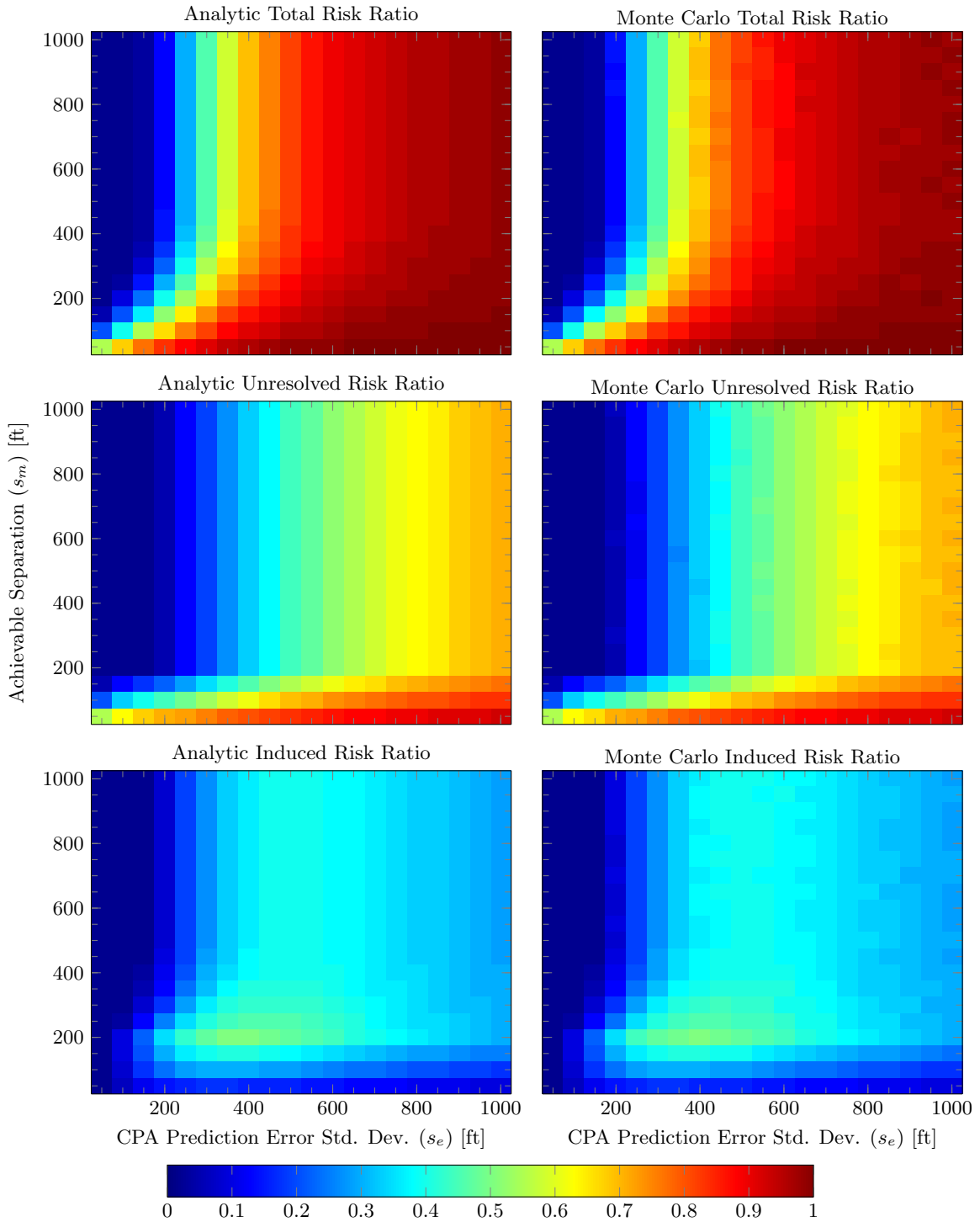


Figure 2. Analytic validation example using Monte Carlo simulation with one million samples ($s_c = 100$ ft, $s_d = 500$ ft).

separation. Therefore, the minimum separation is the minimum distance between this decision point and the cycloid. As depicted in the figure, the achievable separation varies widely based on the encounter geometry

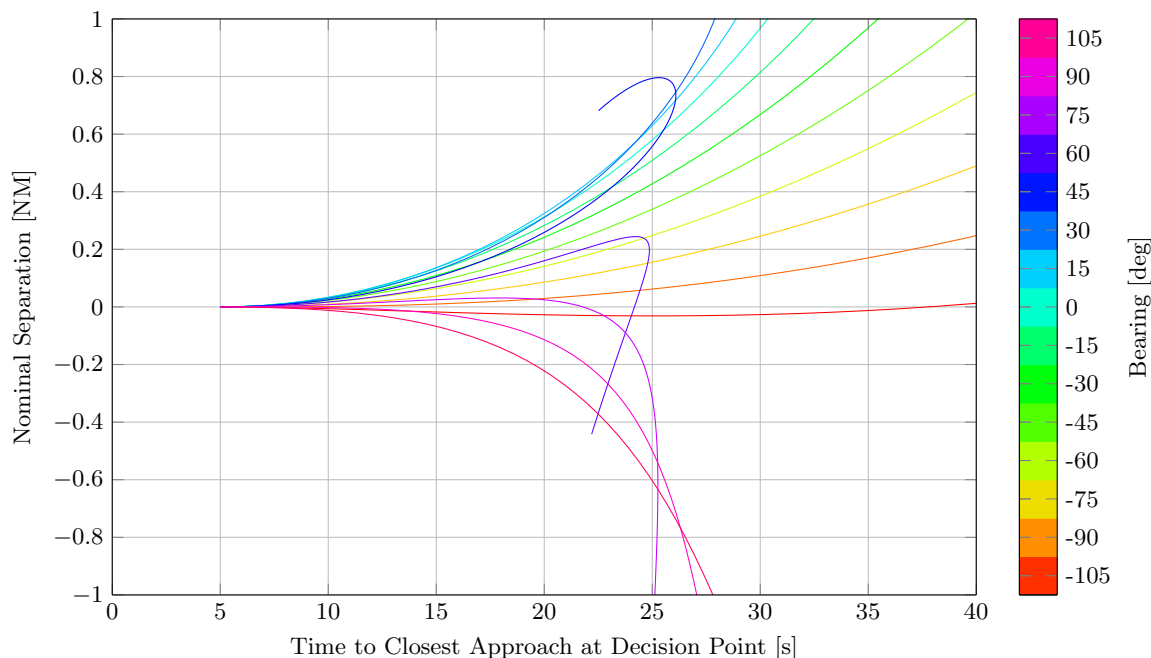


Figure 3. Cycloids for left turning escape maneuver where positive bearings represent a turn away and negative bearings represent a turn towards. Parameters are: 300 kt own speed, 360 kt closing speed, 0.5 g left turn ($1.82^\circ/\text{s}$), 60 s trajectory duration, 5 s response delay.⁹

and when a maneuver is selected; some encounter geometries will have little achievable separation (e.g., -105° bearing), others will achieve relatively large separation (0°), while others will achieve a separation and then decrease separation (60°). This last case represents encounters where the intruding aircraft is passed, but the turn continues such that the aircraft come back into conflict. In this case, it is likely that a turn would not be selected to continue indefinitely; stopping a turn maneuver would be represented by a linear tangent at the appropriate point relative to the cycloid. In general, there are then four maneuver options when selecting a maneuver to maximize separation: indefinite turn left or right, or ceasing the maneuver when the slope of the tangent is greatest. The maneuverability is then defined as the maximum of continuing or ceasing the maneuver, averaged over each direction. Furthermore, it is assumed for simplicity that maneuverability is defined for aircraft on a collision course where there is no nominal separation. The result of this procedure for the same conditions as Figure 3 is shown in Figure 4. This figure also shows an upper bound defined by the own aircraft maneuverability—i.e., it is not possible to increase separation by more than the own total path deviation. The ratio of own to intruder speeds defines the relative shape of the achievable separation response, while a change in the own aircraft speed will only scale the achievable separation given a fixed speed ratio.

F. Closest Separation Estimation Accuracy

Although the closest approach separation accuracy could be imposed as the tracker requirement, the surveillance system designer must be able to trace this requirement to surveillance parameters or there must be a way to derive lower level requirements, such as at the track or sensor state level. Assuming no current or future maneuvering, the horizontal closest approach can be estimated as

$$\text{CPA}_h = \frac{-\dot{\theta}r^2}{v}, \quad (14)$$

where $\dot{\theta}$ is the azimuth rate, r is the range, v is the relative velocity, and all are defined in the horizontal dimension.¹⁰ The relative velocity is defined as $\sqrt{\dot{r}^2 + (\dot{\theta}r)^2}$, where \dot{r} is the range rate. If it is assumed that

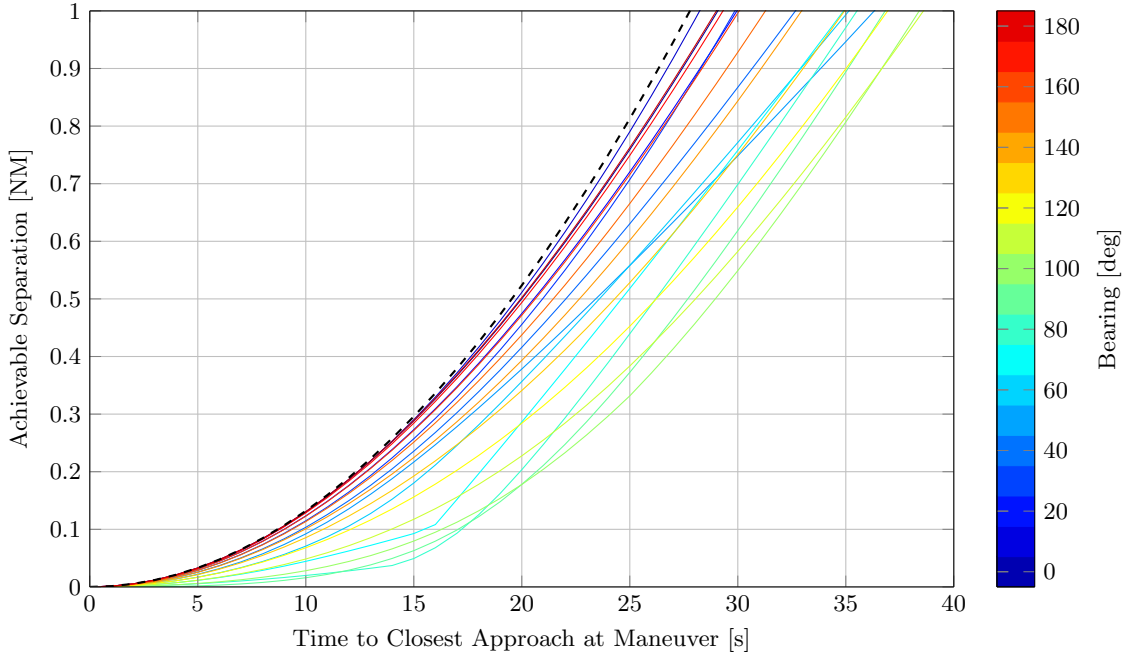


Figure 4. Achievable separation where both turning directions are considered. The dashed black line is the upper bound defined by the own maneuverability. Parameters are: 300 kt own speed, 360 kt closing speed, 0.5 g turn ($1.82^\circ/\text{s}$). Compared to the previous figure, turns are limited to a maximum 90° heading change.

the conflicting aircraft are approximately on a collision course, then the relative velocity can be assumed equivalent to the range rate and the time to collision equivalent to the range normalized by range rate (r/\dot{r}), resulting in

$$\text{CPA}_h \approx \frac{-\dot{\theta}r^2}{\dot{r}} \quad (15)$$

$$\approx -\dot{\theta}t^2\dot{r} \quad (16)$$

The vertical separation at minimum horizontal separation, defined at time t , is

$$\text{CPA}_v = \dot{h}t + h \quad (17)$$

$$= r\dot{\phi}t + r \sin \phi \quad (18)$$

$$\approx \dot{\phi}t^2\dot{r} + \phi t\dot{r} \quad (19)$$

$$\approx \dot{\phi}t^2\dot{r} \quad (20)$$

given the same assumptions as for the horizontal CPA formulation, where h is the relative height, and ϕ is the elevation; due to small elevation angles, $\sin \phi$ can typically be simplified to ϕ . Furthermore, the first term dominates the second term due to the quadratic time dependence such that the second term can largely be ignored, resulting in similar forms for both the vertical and horizontal CPA estimates. Because it is assumed that the terms other than the angle rate are scaling—i.e., not dependent on the value of the angle rate—the standard deviation of the angle rate error is scaled by these terms to obtain the CPA estimate standard deviation—i.e., $\sigma_{\text{CPA}_h} = \sigma_{\dot{\theta}}t^2\dot{r}$.

As was depicted in the previous section (e.g., Figure 4), the achievable separation in the horizontal dimension grows linearly with time after completion of the maneuver; this is also true in the vertical dimension. However, the CPA estimation error grows quadratically with time. This is the fundamental challenge with angle based measurement on the platform, using a sensor such as radar, electro-optic, or infrared: the surveillance errors will overwhelm the achievable separation as time increases. However, this is not true of inertially referenced surveillance, such as that derived from global navigation satellite systems (as in Automatic Dependent Surveillance-Broadcast, or ADS-B), ground based surveillance, or barometric altimetry. In these cases,

the inertial velocity rather than the relative angle rate is estimated, thus resulting in a linear relationship with time and removing the range rate dependence—e.g., as in Equation 17. Therefore, the increase in CPA prediction error is counteracted directly with the ability to maneuver; however, the maneuver magnitude required to overcome the surveillance uncertainty may not be desirable. Furthermore, any transmission or response delays will exacerbate the challenge because there is less maneuver time, and thus achievable separation, for the same prediction uncertainty. Stated another way, the prediction uncertainty will be larger for the same maneuver time. These challenges are illustrated in Figure 5 (see also corresponding Matlab code for generating this figure in the appendix). With arbitrary maneuver magnitudes (maneuver indefinitely), the risk ratio response is asymptotic for inertial surveillance, while relative surveillance will asymptotically approach unity. When a desired separation is specified, the risk for both surveillance reference frames will approach unity as the maneuver time is increased.

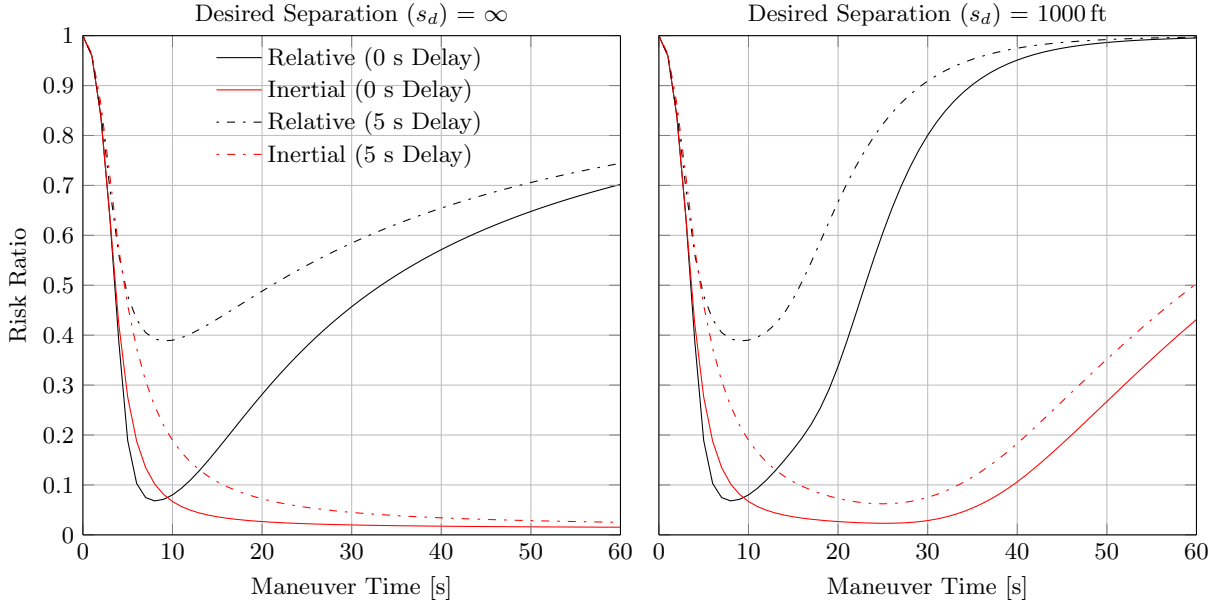


Figure 5. Example risk ratio response for relative (angle based) and inertial referenced surveillance with and without delays. Parameters: 360 kt closing speed, standard TCAS vertical response (1500 ft/min at 1/4 g acceleration), $s_c = 100$ ft, desired separation as shown, $\sigma_{\dot{\theta}} = 0.1^\circ/\text{s}$ for relative, $\sigma_{\dot{h}} = 10$ ft/s for inertial, only rate terms are considered (not position error).

The filtered/tracked surveillance error has been the focus thus far, but it could be useful to decompose a level further to the sensor state level. If a first-order recursive least-squares estimator is assumed where the signal and its derivative are estimated (e.g., angle and angle rate), the standard deviations of the filtered errors are as follows (also for a Kalman filter without process noise):¹¹

$$\sigma_{\theta} = \sigma_{\theta_r} \sqrt{\frac{2(2k-1)}{k(k+1)}}, \quad (21)$$

$$\sigma_{\dot{\theta}} = \frac{\sigma_{\theta_r}}{T_s} \sqrt{\frac{12}{k(k^2-1)}}, \quad (22)$$

where σ_{θ_r} is the raw surveillance standard deviation, k is the number of independent measurements used within the filter, and T_s is the time between measurements; the azimuth, θ , could be substituted by any measurement—e.g., elevation, range, altitude. Note that although it would appear from these equations that the estimates can be refined indefinitely, a filter in practice will effectively limit the number of measurements used to account for maneuvering and other modeling errors.

G. Airspace Environment Consideration

Encounters are experienced at a range of environmental conditions that influence risk, but it is desirable to characterize the average risk. This is contrasted with evaluating risk at a worst or typical case where these cases may not be obvious or representative. For Air Traffic Management (ATM) systems, risk is typically evaluated as an average measure: estimating risk as an average over the expected distribution of encounter conditions is consistent with existing ATM systems, such as TCAS and ADS-B, where surveillance uncertainty and encounter geometry distributions are considered. However, these systems are often tuned to ensure consistent risk across operational conditions that have substantively different surveillance accuracy where practicable. For example, the TCAS desired separation (ALIM) changes with altitude to ensure a consistent risk as barometric altimeter system error increases with altitude, and Air Traffic Control (ATC) separation standards depend on the surveillance accuracy—e.g., 3 and 5 NM separation based on radar accuracy. Furthermore, averaging may mask deficient performance at a specific condition, so individual conditions should also be considered. Although this approach of using distributions to assess average performance is typically used to evaluate measurement accuracy characteristics and requirements, deterministic requirements such as detection and tracking range are often set for the worst case anticipated configuration. This ensures that there is adequate time to respond for all anticipated encounters—for example, the TCAS tracking range requirement is based on worst case closing speed that varies based on altitude (above and below 10,000 ft AGL).

An overall average estimate of the system performance requires consideration of the encounter likelihood, as defined by aircraft speed and relative geometry, as well as other variables that may affect system efficacy such as those that affect surveillance accuracy or achievable separation. In general terms, the average risk ratio is

$$\text{RR}_{\text{avg}} = \int \text{RR}_{\text{enc}} p(\text{RR}_{\text{enc}}) d\text{RR}_{\text{enc}}, \quad (23)$$

where RR is the risk ratio, enc is an encounter condition, and the encounter risk ratio probability is the likelihood of encountering that condition:

$$p(\text{RR}_{\text{enc}}) = p(v_o, v_i, \psi, \text{enc}) \quad (24)$$

$$= p(\text{enc} | v_o, v_i, \psi) p(v_o, v_i, \psi), \quad (25)$$

where v_o and v_i are the speeds for the own and intruder aircraft, respectively, and ψ is the relative heading. The airspeed and relative heading probabilities are independent such that the joint distribution is simply the product of each probability. These probabilities may be derived from an encounter model that represents the statistical likelihood of encounter and aircraft properties.¹² The conditional encounter probability considers that aircraft pairs with higher relative speeds are more likely to come into conflict, that is

$$p(\text{enc} | v_o, v_i, \psi) = v_r = \sqrt{v_o^2 + v_i^2 - 2v_o v_i \cos \psi}. \quad (26)$$

Because the probability distributions over v_o and v_i are not represented by continuous distributions in the encounter model, the average risk ratio must be numerically computed:

$$\text{RR}_{\text{avg}} = \frac{\sum_{\text{enc}} \text{RR}_{\text{enc}} v_r p(v_o) p(v_i) p(\psi)}{\sum_{\text{enc}} v_r p(v_o) p(v_i) p(\psi)}. \quad (27)$$

When aircraft blunder into close proximity in an unstructured manner, the relative heading distribution is uniform such that this term may be dropped from Equation 27. As shown in the previous sections, the risk ratio during a given encounter is not constant and depends on many factors. Therefore, the risk ratio for a given encounter must be carefully selected by considering how the system is employed: for example, it may be useful to assess the minimum, maximum, or average achievable risk ratio during an encounter. Furthermore, there are likely to be different risks when maneuvering horizontally versus vertically. These risks could be analyzed separately to evaluate their relative efficacy, or combined at the encounter level to evaluate the combined efficacy. Lastly, it may also be useful to consider the altitude dependence of risk: the encounter conditions as well as the achievable separation and surveillance accuracy may vary by altitude. The risk ratio could be analyzed for each altitude separately, or if the distribution of altitude for both aircraft was known, then it could be considered within the average risk ratio in a similar manner as the other encounter conditions accounted for above.

III. Results

The following results provide an example of implementing the methodology presented by mapping surveillance uncertainty to the risk ratio and alerting performance for an unmanned aircraft with SAA encountering uncorrelated traffic: uncorrelated encounters are those without air traffic control intervention, such as between a controlled aircraft and a noncooperative, or nontransponding, intruder.¹² Because aircraft above 10,000 ft are required to carry transponding equipment, uncorrelated encounters are expected primarily below this altitude (14 CFR §91.215). Due the wide range of anticipated unmanned aircraft performance, a range of speeds (50–250 kt) and avoidance maneuvers are considered: avoidance maneuvers are assumed to be vertical or horizontal here, but combination and speed change maneuvers could also be considered. For avoidance maneuvers, both slow and fast responses are considered: half ($1.5^\circ/\text{s}$) and full ($3^\circ/\text{s}$) standard rate turns, and 500 and 1500 ft/min (consistent with TCAS) vertical rates, for slow and fast responses, respectively. Lastly, a sensor using angle-of-arrival measurements to estimate cross range velocity is assumed, where this cross range velocity is the major contribution to the future state uncertainty such that other sources can be ignored; an airborne primary radar is an example of such a sensor. Before the risk ratio and alerting results are shown, the uncorrelated environment is described, followed by the achievable separation in this environment.

A. Uncorrelated Environment

The uncorrelated environment is defined by a National Airspace System (NAS) uncorrelated encounter model, which was built using a national collection of air traffic control radars.¹³ The uncorrelated model assumes unstructured encounters, such that aircraft blunder into close proximity without prior coordination. The uncorrelated model essentially captures the characteristics of individual aircraft in the environment, then combines the aircraft into encounters such that the effect of the SAA system of interest can be evaluated. Figure 6 illustrates the main encounter model characteristics applicable to these results: relative heading and relative velocity.

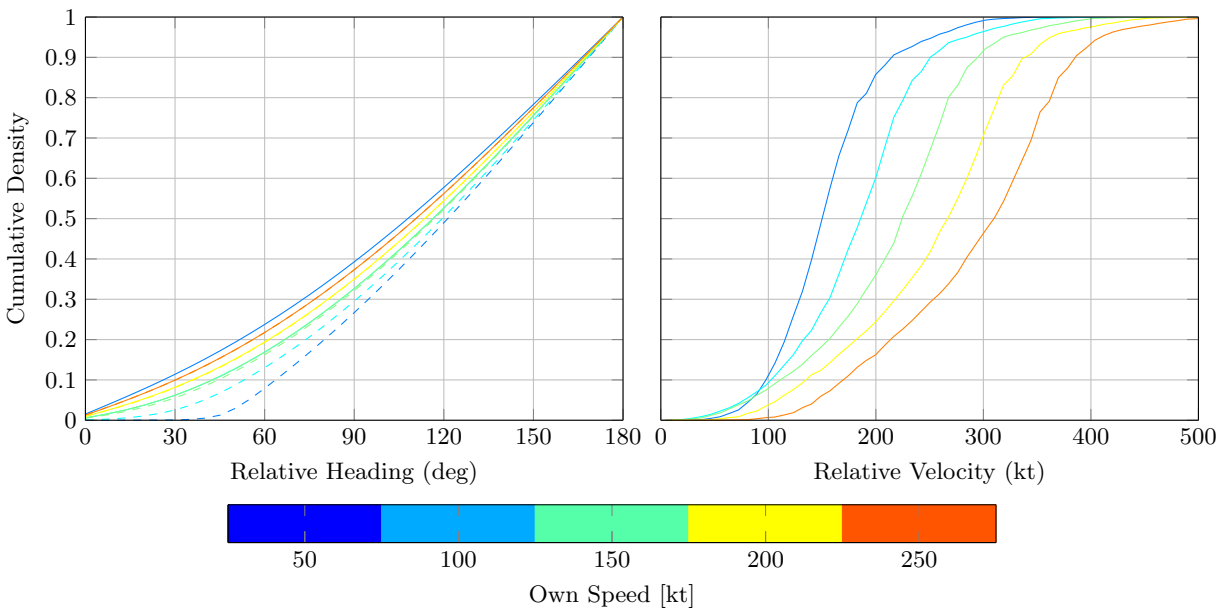


Figure 6. Relative heading and velocity distributions given an uncorrelated encounter. Dashed lines for the relative heading distribution represent encounters only considered in the field of regard ($<110^\circ$ azimuth), while the solid lines represent all geometries.

B. Achievable Separation

The achievable separation (maneuverability) given an uncorrelated encounter is presented in Figure 7, considering the likelihood of the encounter geometry from the encounter model (as shown in Figure 6). Because this considers the likelihood of encounters, this is an average; thus, there are encounters with significantly more or less achievable separation. There are two main features that are of note: first, if there is sufficient maneuver time, horizontal maneuvers provide more separation than vertical; second, higher ownship speeds and turn rates provide more separation, as expected. For horizontal maneuvers, separation increases quadratically until the maneuver is complete, and then there is nonaccelerating relative motion.

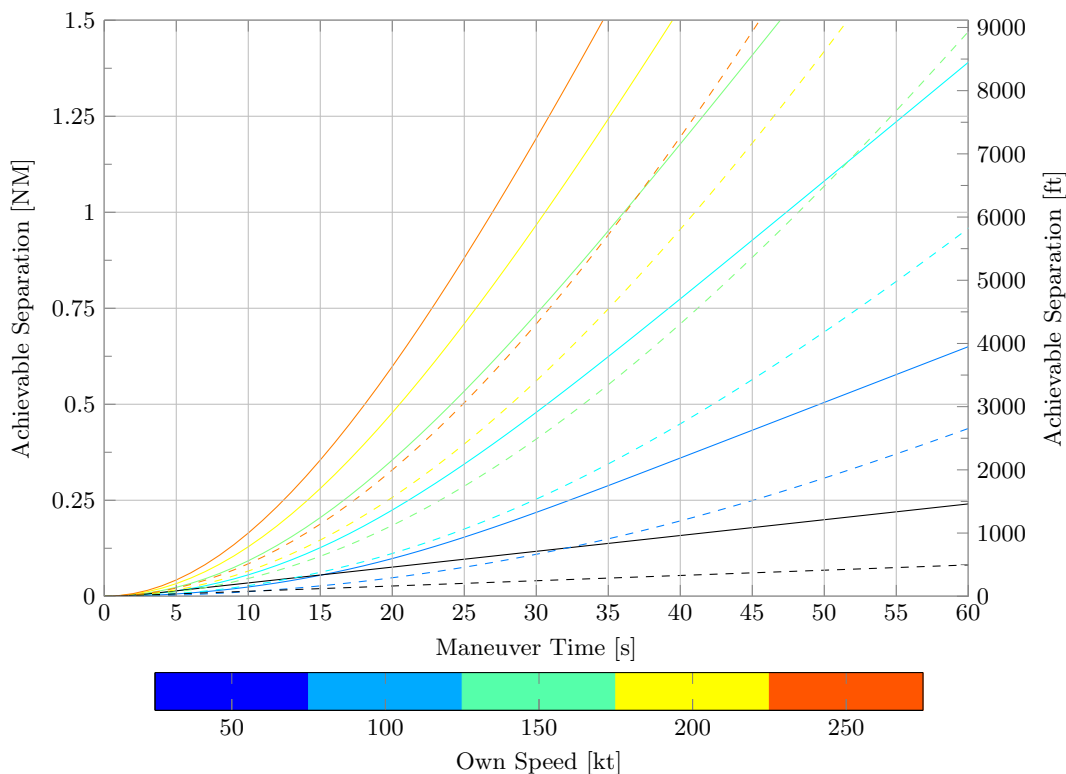


Figure 7. Average horizontal (colored) and vertical (black) achievable separation for fast (solid) and slow (dashed) responses.

C. Risk Ratio

Based on the achievable separation, the risk ratio can be assessed for sensitivity to the cross range velocity error, parameterized here in terms of angular rate standard deviation (Figure 8). The conflict definition used here is that used for TCAS collision risk analysis: a near midair collision (NMAC) defined as separation less 500 ft horizontally and 100 ft vertically.⁴ The single maneuver decision is assumed at 30, 60, or 90 seconds prior to closest approach, with 5 s response delay. Due to the relatively small separation achievable vertically, the vertical angular rate uncertainty required to achieve the same risk ratio is much smaller than that required horizontally (approximately one order of magnitude). Thus, horizontal maneuvers will be more effective for the same angular rate uncertainty. Additionally, vertical maneuvers require better accuracy for larger decision times; horizontally, it is not as straightforward due to the complex nature of horizontal maneuvers where different geometries (relative headings) can have significant variability in achievable separation (recall Figure 4). Horizontal and vertical maneuvers display opposing sensitivity to own aircraft speed: horizontal maneuvers require better accuracy for slower speeds, while the opposite is true vertically. This effect is due to vertical separation being assumed independent of own aircraft speed, while horizontal separation is very sensitive to own speed (Figure 7). This is especially pronounced for the 50 kt half rate turn ($1.5^\circ/s$) scenario

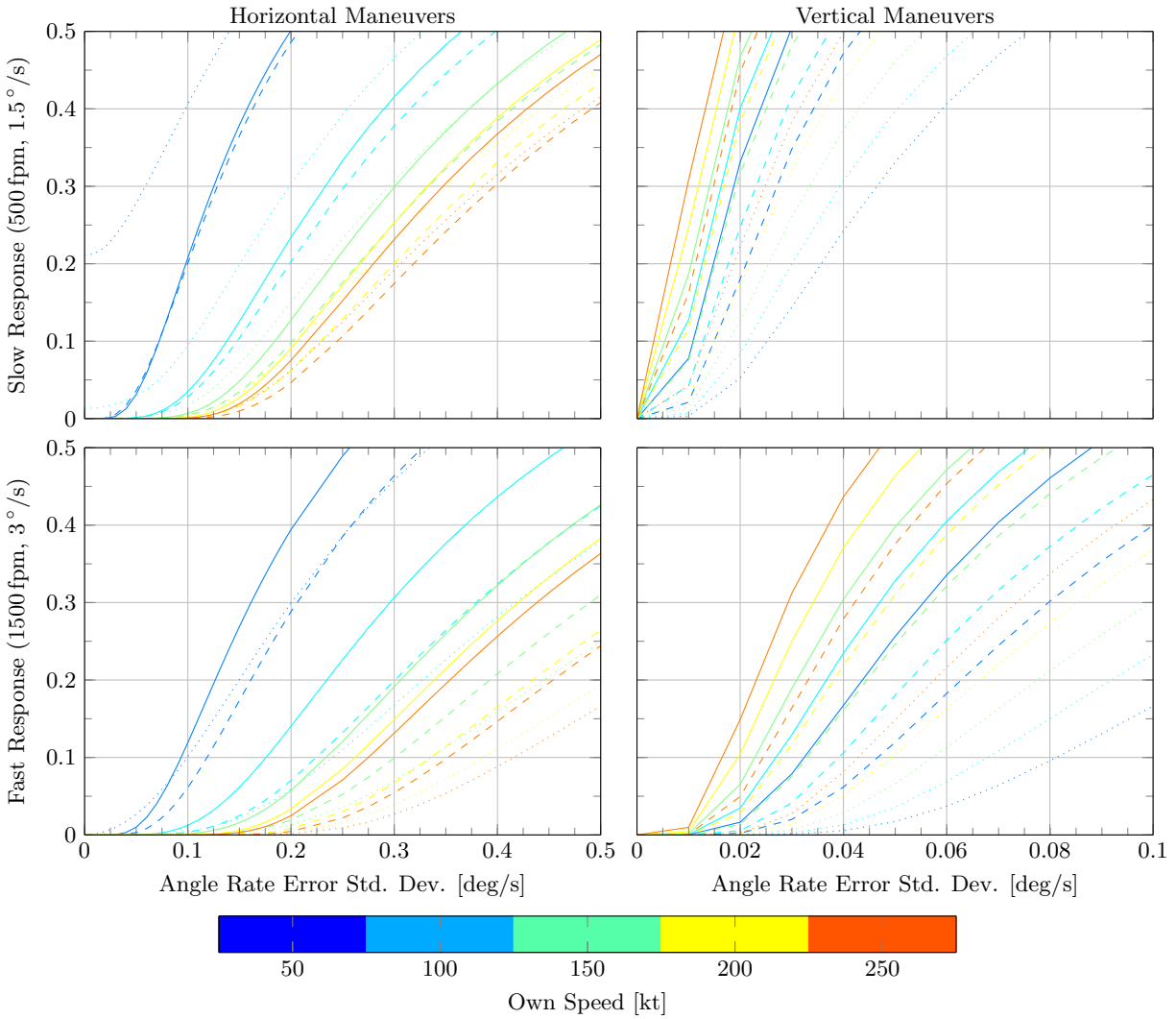


Figure 8. Average risk ratio sensitivity at 30 s (dotted lines), 60 s (dashed lines), and 90 s (solid lines) decision times to angle rate error, response rates, and own speed for vertical and horizontal maneuvers. Note that the vertical risk ratio plots have a reduced angle rate error range to highlight the lower risk ratio portion of the figure. Parameters: infinite desired separation, 5 s response delay.

where the risk ratio with no uncertainty is nonzero because there are some geometries with 30 s decision time where the achievable separation is less than the conflict definition (500 ft).

D. Alerting Performance

An SAA system may not be required to maneuver in both dimensions—e.g., the risk ratio results show that it may be difficult to make effective maneuvers vertically using relative surveillance. Therefore, the surveillance performance in the nonmaneuvering dimension must be sufficient to enable detection, but not avoidance, of the threat. The metric used to assess the performance of threat detection is the missed detection ratio (MDR), and the results are shown in Figure 9. The MDR calculation (Equation 10) assumes that there is a threshold displacement around the aircraft where a threat is declared if the intruder is predicted to penetrate the threshold (s_b). Although it would seem that s_b could be made arbitrarily large, it must be traded with increasing the nuisance alert rate (results not shown here). Also, note that these results are independent of the achievable separation; therefore, if the missed detection and conflict thresholds were the same for vertical and horizontal dimensions, the resulting MDR sensitivity would be the same. These results

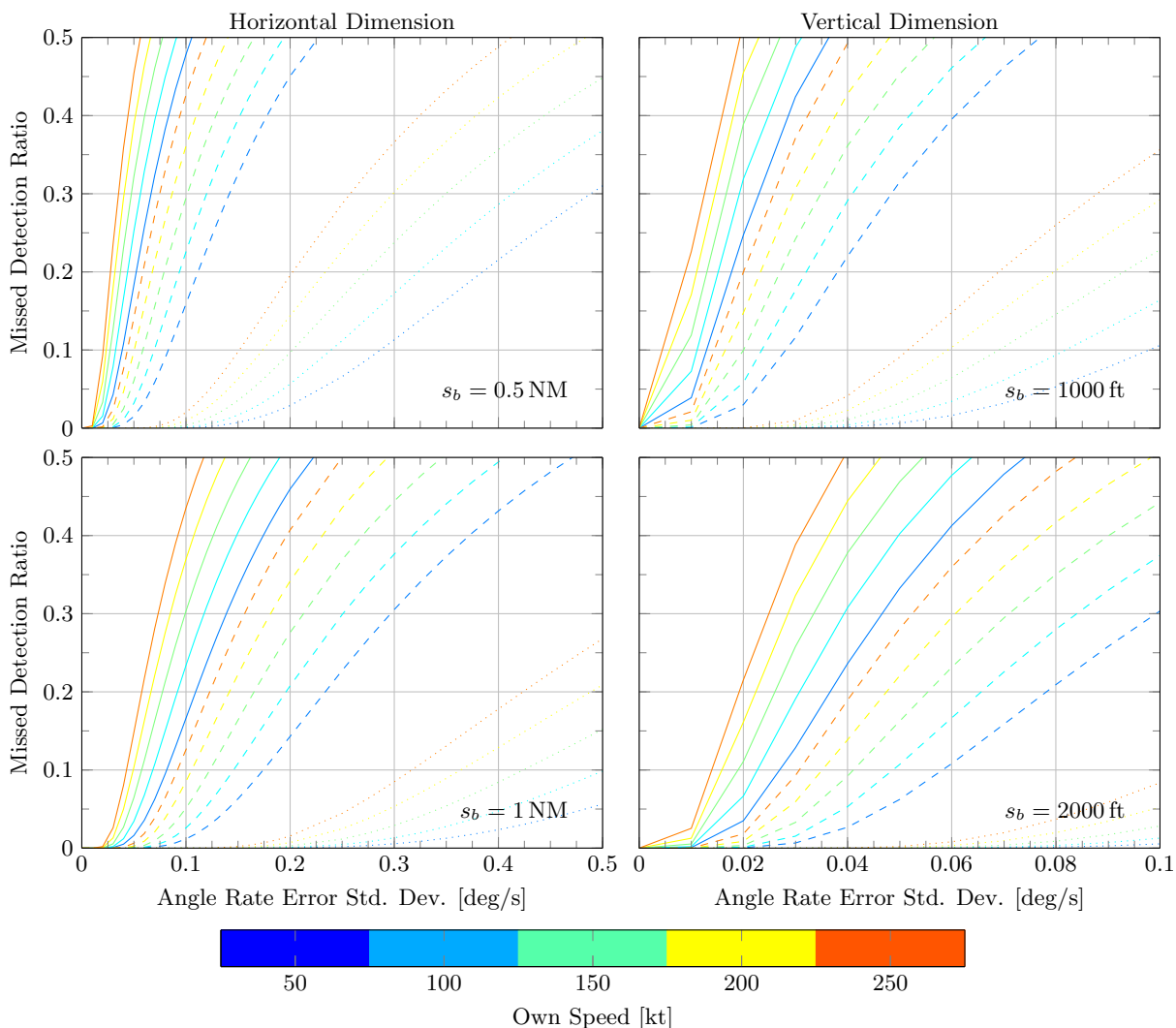


Figure 9. Missed detection ratio sensitivity at 30 s (dotted lines), 60 s (dashed lines), and 90 s (solid lines) decision times to angle rate error and own speed for vertical and horizontal dimensions. Note that the vertical MDR plots have a reduced angle rate error range to highlight the lower angular rate portion of the figure. Parameters: 5 s response delay, MDR boundary (s_b) as shown.

show that the larger the decision time (and thus range), the better accuracy is required to achieve the same missed detection performance. Both vertical and horizontal results are consistent in that higher own speeds require better accuracy for the same MDR because the state must be propagated at greater ranges (for the same time to closest approach).

IV. Conclusion

This paper outlined a method for evaluating the sense and avoid surveillance contribution to safety using an alternative approach to existing resource intensive Monte Carlo (sample based) simulation methods. This simpler approach parameterizes the collision avoidance problem analytically, thereby mitigating the computational requirements and enabling key insights into the collision avoidance challenges. Specifically, it was shown that the ability to predict the relative encounter state at the closest point of approach drives collision risk. For surveillance systems that measure angle relative to the aircraft platform such as airborne radar, this closest approach accuracy is directly proportional to the tracked angle rate accuracy, the range rate, and the

square of the time to collision. Therefore, the key challenge to collision avoidance using relative surveillance is that the ability to maneuver increases linearly with time while the ability to predict the future state of the encounter degrades quadratically with time. When coupled with a probabilistic characterization of the environment, this approach yields the average risk in the environment. This approach was demonstrated by assessing the safety sensitivity to track uncertainty for unmanned aircraft with varying performance characteristics when encountering uncorrelated traffic, such as noncooperative aircraft. Although this approach provides direct, analytic traceability between collision risk and surveillance performance that will prove useful throughout system development, Monte Carlo simulation methods remain necessary for system validation and verification in order to fully capture the surveillance system details, including actual sensor and tracker performance, and other system components, such as threat logic and maneuver guidance.

Follow-on work is recommended to refine and validate the approach:

- Consideration of other surveillance collision risk contributors, specifically those influencing detection performance such as power-aperture, intruder signature, and clutter.
- Development of an approach for defining and verifying required surveillance performance requirements in terms of performance based requirements rather than equipment (sensor) specific requirements.
- Incorporation of intruder future state uncertainty using encounter models. Encounter models were only used here to assess the likelihood of the encounter geometry (speed and relative heading).
- Consideration of additional sensors modalities, including ADS-B and TCAS cooperative surveillance and Electro-Optical and Infrared noncooperative surveillance.
- Consideration of multiple maneuvers and their potential benefits and drawbacks.
- Evaluation of operational suitability metrics beyond alerting rate, including considerations such as crossing maneuvers and following the right of way rules.
- Development and evaluation of methods for integrating the analytic approach into recommended maneuver selection and alerting. For example, this approach could judge the relative efficacy of vertical and horizontal maneuvers, and evaluate whether it is prudent to make a maneuver decision or to wait until there is a better track estimate.

References

- ¹Edwards, M. W. M., “A Safety Driven Approach to the Development of an Airborne Sense and Avoid System,” *In-fotech@Aerospace*, No. AIAA 2012-2485, AIAA, Garden Grove, California, June 2012.
- ²Kuchar, J. K., “Safety Analysis Methodology for Unmanned Aerial Vehicle Collision Avoidance Systems,” *ATM Seminar*, Baltimore, Maryland, June 2005.
- ³Jamoom, M. B., Joerger, M., and Pervan, B., “Unmanned Aircraft System Sense-and-Avoid Integrity and Continuity Risk,” *Journal of Guidance, Control, and Dynamics*, Vol. 39, No. 3, 2016, pp. 498–509.
- ⁴RTCA, “Minimum Operational Performance Standards for Traffic Alert and Collision Avoidance System II,” DO-185B, 2008.
- ⁵Lebron, J. E., Zeitlin, A. D., Spencer, N. A., Andrews, J. W., and Harman, W. H., “System Safety Study of Minimum TCAS II,” Tech. Rep. DOT/FAA/PM-83/36, MITRE and MIT Lincoln Laboratory, 1983.
- ⁶Kochenderfer, M. J., Griffith, J. D., and Olszta, J. E., “On Estimating Mid-Air Collision Risk,” *10th AIAA Aviation Technology, Integration, and Operations Conference*, No. AIAA 2010-9333, AIAA, Fort Worth, Texas, September 2010.
- ⁷International Civil Aviation Organization, “Surveillance, radar and collision avoidance,” *International Standards and Recommended Practices*, Vol. IV, Annex 10, 4th ed., July 2007.
- ⁸Hutchinson, H. J., “ACAS Safety Analysis post-RVSM: Update of altimetry-error assumptions,” Tech. Rep. ASARP/WP3/16/D, Eurocontrol, 2006.
- ⁹Morrel, J. S., “The Mathematics of Collision Avoidance in the Air,” *Journal of Navigation*, Vol. 11, No. 1, 1 1958, pp. 18–28.
- ¹⁰Morrel, J. S., “The Use of Self-contained Range and Azimuth Measuring Apparatus to Detect Collision Courses,” *Journal of Navigation*, Vol. 11, No. 3, 7 1958, pp. 318–321.
- ¹¹Zarchan, P. and Musoff, H., *Fundamentals of Kalman Filtering: A Practical Approach*, Vol. 190 of *Progress in Astronautics and Aeronautics*, American Institute of Aeronautics and Astronautics, Inc., Reston, Virginia, 2000.
- ¹²Kochenderfer, M. J., Edwards, M. W., Espindle, L. P., Kuchar, J. K., and Griffith, J. D., “Airspace Encounter Models for Estimating Collision Risk,” *Journal of Guidance, Control, and Dynamics*, Vol. 33, No. 2, 2010, pp. 487–499.
- ¹³Weinert, A. J., Harkleroad, E. P., Griffith, J. D., Edwards, M. W., and Kochenderfer, M. J., “Uncorrelated Encounter Model of the National Airspace System Version 2.0,” Project Report ATC-404, Massachusetts Institute of Technology, Lincoln Laboratory, 2013.

Analytic Solution Matlab Code

The following Matlab code solves the equations in Sections II.A and II.B.

```
% Purpose: generate the unresolved and induced analytic solutions and
% compute example
clear all;
%% Analytic solution
% Define symbols
syms s_d s_c s_m s_b s_n s_indmax pi sigma positive
syms s_e s_a real

% Error distribution
p = 1/sigma/sqrt(2*pi)*exp(-s_e^2/2/sigma^2); % Probability density for normal distribution

% Unresolved Risk Ratio
% s_m > 2*s_c
RR_unresolved_smg2sc = 2*int(p,s_e,s_d-s_c,inf);
% s_c > s_m
RR_unresolved_scgsm = 1-1/(2*s_c)*2*int(int(p,s_e,-s_a,s_d-s_c),s_a,abs(s_m-s_c),s_c);
% 2*s_c > s_m > s_c
RR_unresolved_2scgsmgsc = 1-1/(2*s_c)*2*int(int(p,s_e,-s_a,s_d-s_c),s_a,abs(s_m-s_c),s_c)-...
    1/(2*s_c)*4*int(int(p,s_e,0,abs(s_d-s_c)),s_a,0,abs(s_m-s_c));

% Induced Risk Ratio
RR_induced_firstterm = 1/(2*s_c)*2*int(int(p,s_e,s_d-s_c,s_d+s_c),s_a,s_c,s_m-s_c);
RR_induced_secondterm = 1/(2*s_c)*2*int(int(p,s_e,s_a,s_d+s_c),s_a,s_indmax,s_m+s_c);

% Alert Ratio
AR = 1/(2*s_c)*int(int(p,s_e,s_a-s_d,s_a+s_d),s_a,-inf,inf);

% Missed Detection Ratio
MDR = 1/(2*s_c)*2*int(int(p,s_e,s_b-s_a,inf),s_a,-s_c,s_c);

% Nuisance Alert Ratio
NAR = 1/(2*s_c)*2*int(int(p,s_e,s_a-s_d,s_a+s_d),s_a,s_n,inf);

%% Example
clear pi
s_c = 100; % Conflict definition
s_d = 500; % Desired separation
s_m = 300; % Achievable separation
s_b = 1000; % Missed detection separation
s_n = 2000; % Nuisance alert separation
sigma = 200; % Standard deviation for Gaussian distribution

s_m = min(s_m,s_d);

% Unresolved Risk Ratio
if s_m > 2*s_c
    RR_unresolved = eval(RR_unresolved_smg2sc);
elseif s_c > s_m
    RR_unresolved = eval(RR_unresolved_scgsm);
elseif 2*s_c > s_m && s_m > s_c
    RR_unresolved = eval(RR_unresolved_2scgsmgsc);
end

% Induced Risk Ratio
s_indmax = max(s_m-s_c,s_c);
if s_c > (s_m - s_c)
    RR_induced_firstterm = sym(0);
end
RR_induced = eval(RR_induced_firstterm)+eval(RR_induced_secondterm);

% Total Risk Ratio
RiskRatio = RR_induced+RR_unresolved;

% Alert Ratio
AlertRatio = eval(AR);

% Missed Detection Ratio
MissedDetectionRatio = eval(MDR);

% Nuisance Alert Ratio
NuisanceAlertRatio = eval(NAR);
```

This script will generate Figure 5, and calls the function listed on the next page.

```

% Purpose: to compare risk using relative angle and inertial surveillance
clear all;

% Constants
NM2ft = 6076.115; % Nautical mile to ft conversion
kt2ftps = 1.68780986; % Knot to ft/s conversion
g = 32.17; % Gravitational acceleration (ft/s^2)

% Sensor characteristics
hdotsigma = 10; % Vertical rate standard deviation (ft/s)
eldotsigma = 0.1*pi/180; % Elevation rate standard deviation (rad/s)
rr = 360*kt2ftps; % Range rate (ft/s)

% Maneuver options
s_c = 100; % Vertical conflict definition (ft)
s_d = inf; % Desired separation (make inf for minimum risk ratio)
dh = 1500/60; % Vertical rate (ft/s)

time = 0:1:60; % Time (s)

% Vertical response
a = 0.25*g; % Acceleration response (ft/s^2)
tresdh = dh/a; % Time at which vertical rate achieved (s)
presdh = 0.5*a*tresdh^2; % Vertical position when vertical rate achieved (ft)
h = time'.*0;
h(time<=tresdh) = 0.5*a*time(time<=tresdh).^2;
h(time>tresdh) = dh*(time(time>tresdh)-tresdh)+presdh;
s_m = h;

% CPA prediction error (assume only based on rates)
cpasigmaeldot = eldotsigma.*time.^2.*rr;
cpasigmahdot = hdotsigma.*time;

% Consider delay
tdelay = 5;
cpasigmaazd = eldotsigma.*(time+tdelay).^2.*rr;
cpasigmahdotd = hdotsigma.*(time+tdelay);

% Get risk ratios
for ii = 1:length(time)
    riskratioaz(ii) = radaracccomp(s_m(ii),s_d,s_c,cpasigmaeldot(ii));
    riskratiohdot(ii) = radaracccomp(s_m(ii),s_d,s_c,cpasigmahdot(ii));
    riskratioazd(ii) = radaracccomp(s_m(ii),s_d,s_c,cpasigmaazd(ii));
    riskratiohdotd(ii) = radaracccomp(s_m(ii),s_d,s_c,cpasigmahdotd(ii));
end

% Plot results
figure;
plot(time,riskratioaz,'k',time,riskratiohdot,'r',...
      time,riskratioazd,'k-.',time,riskratiohdotd,'r-.');
xlabel('Maneuver Time (s)')
ylabel('Risk Ratio')
legend('Relative (0 s Delay)', 'Inertial (0 s Delay)',...
      'Relative (5 s Delay)', 'Inertial (5 s Delay)',...
      'Location', 'Best')

```

This function will calculate the risk ratio and alert ratio assuming a Gaussian distribution (as calculated in the first script listed).

```
function [RiskRatio,RR_unresolved,RR_induced,AlertRatio] = radaracccomp(s_m,s_d,s_c,sigma)
%RADARACCCOMP function to compute risk ratios given maneuver options
% This function will compute the risk ratio given maneuverability, desired
% separation, accuracy; assumes Gaussian distributed closest point of
% approach error
%
% Outputs:
% RiskRatio - total risk ratio
% RR_unresolved - unresolved component of risk ratio
% RR_induced - induced component of risk ratio
%
% Inputs:
% s_m - achievable separation
% s_d - desired separation
% s_c - conflict definition
% sigma - standard deviation of CPA estimation error (Gaussian dist.)

s_m = min(s_m,s_d);

% Unresolved Risk Ratio
if s_m > 2*s_c
    RR_unresolved = erf((2^(1/2)*(s_c - s_d))/(2*sigma)) + 1;
elseif s_c > s_m
    RR_unresolved = 1 - ((s_c*erf((2^(1/2)*s_c)/(2*sigma)))/2 + (abs(s_c - s_m)*erf((2^(1/2)*(s_c/2 - s_d/2))/sigma))/2 - ...
        (abs(s_c - s_m)*erf((2^(1/2)*abs(s_c - s_m))/(2*sigma)))/2 - (s_c*erf((2^(1/2)*(s_c/2 - s_d/2))/sigma))/2 - ...
        (sigma*exp(-abs(s_c - s_m)^2/(2*sigma^2))*(2/pi)^(1/2))/2 + (sigma*exp(-s_c^2/(2*sigma^2))*(2/pi)^(1/2))/2)/s_c;
elseif 2*s_c > s_m && s_m > s_c
    RR_unresolved = 1 - (abs(s_c - s_m)*erf((2^(1/2)*abs(s_c - s_d))/(2*sigma)))/s_c - ...
        ((s_c*erf((2^(1/2)*s_c)/(2*sigma)))/2 + (abs(s_c - s_m)*erf((2^(1/2)*(s_c/2 - s_d/2))/sigma))/2 - (abs(s_c - ...
        s_m)*erf((2^(1/2)*abs(s_c - s_m))/(2*sigma)))/2 - (s_c*erf((2^(1/2)*(s_c/2 - s_d/2))/sigma))/2 - ...
        (sigma*exp(-abs(s_c - s_m)^2/(2*sigma^2))*(2/pi)^(1/2))/2 + (sigma*exp(-s_c^2/(2*sigma^2))*(2/pi)^(1/2))/2)/s_c;
end

% Induced Risk Ratio
s_indmax = max(s_m-s_c,s_c);
if s_c > (s_m - s_c)
    RR_induced_firstterm = 0;
else
    RR_induced_firstterm = -((2*s_c - s_m)*erf((2^(1/2)*(s_c + s_d))/(2*sigma)) + erf((2^(1/2)*(s_c - ...
        s_d))/(2*sigma)))/(2*s_c);
end
RR_induced_secondterm = ((s_indmax*erf((2^(1/2)*s_indmax)/(2*sigma)))/2 + (erf((2^(1/2)*(s_c/2 + s_d/2))/sigma)*(s_c + ...
    s_m)/2 - (erf((2^(1/2)*(s_c/2 + s_m/2))/sigma)*(s_c + s_m)/2 - (s_indmax*erf((2^(1/2)*(s_c/2 + s_d/2))/sigma))/2 - ...
    (sigma*exp(-(s_c + s_m)^2/(2*sigma^2))*(2/pi)^(1/2))/2 + (sigma*exp(-s_indmax^2/(2*sigma^2))*(2/pi)^(1/2))/2)/s_c;
RR_induced = RR_induced_firstterm+RR_induced_secondterm;

% Total Risk Ratio
RiskRatio = RR_induced+RR_unresolved;

% Alert Ratio
AlertRatio = s_d/s_c;
```